# Bipyridil-based chelator for Gd(III) complexation: kinetic, structural and relaxation properties

Szilvia Bunda,[§] Norbert Lihi,[†*] Zsófia Szaniszló,[§] David Esteban-Gómez,[‡] Carlos Platas-Iglesias,[‡*] Mónika Kéri,[§] Gábor Papp[§] and Ferenc Krisztián Kálmán[§*]

[§] Department of Physical Chemistry, Faculty of Science and Technology, University of Debrecen, H-4032 Debrecen, Hungary

[†] HUN-REN–UD Mechanisms of Complex Homogeneous and Heterogeneous Chemical Reactions Research Group, Department of Inorganic and Analytical Chemistry, Faculty of Science and Technology, University of Debrecen, H-4032 Debrecen, Hungary

[‡] Centro Interdisciplinar de Química e Bioloxía (CICA) and Departamento de Química, Facultade de Ciencias, Universidade da Coruña, 15071 A Coruña, Galicia, Spain

**Abstract:**

In the last 20 years, the research in the field of MRI (magnetic resonance imaging) contrast agents (CA) has been intensified again related to the appearance of a disease called nephrogenic systemic fibrosis (NSF). NSF was linked to the *in vivo* dissociation of certain Gd(III)-based compounds applied in MRI as CAs. To prevent the dechelation of the probes after the intravenous injection, the improvement of their *in vivo* stability is highly desired. The inertness of the Gd(III) chelates can be increased due to the rigidification of the ligand structure. One of the potential ligands is the (2,2',2'',2'''-(((2,2'-bipyridine]-6,6'-diylbis(methylene))bis(azanetriyl))tetraacetic acid) ( ) successfully used as fluorescent probe for lanthanides, however, it has never been considered as potential chelator for Gd(III) ion.

In this paper, we report the thermodynamic, kinetic and structural features of the complex formed between Gd(III) and DIPTA. Since, the solubility of the $[Gd(DIPTA)]^-$ chelate is very low in acidic condition hampering the thermodynamic characterization, we can only assume that its stability is close to the one determined for the structurally analogue $[Gd(FENTA)]^-$ ( : (1,10-phenanthroline-2,9-diyl)bis(methyliminodiacetic acid)) which is similar to that determined for the agent $[Gd(DTPA)]^{2-}$ routinely used in the clinical practice.

Unfortunately, the inertness of the $[Gd(DIPTA)]^-$ is significantly lower ($_{/2}=1.34$ h), than that was obtained for the $[Gd(EGTA)]^-$ and $[Gd(DTPA)]^{2-}$ as a result of the spontaneous dissociation pathway in its dechelation. The relaxivity values of $[Gd(DIPTA)]^-$ are comparable with those of the $[Gd(FENTA)]^-$ and somewhat higher than the values characterizing the $[Gd(DTPA)]^{2-}$. The luminescence lifetime measurements indicate the presence of one water molecule ($q=1$) in the inner sphere of the complex with a relatively high water exchange rate ($=43(5)\times$ $s^{-1}$). The DFT calculations suggest a rigid distorted tricapped trigonal prism polyhedron for the Gd(III) complex. On the basis of these results, we can conclude that the bipyridine backbone is not favourable with respect to the inertness of the chelate.

## Introduction

Research to develop safe Magnetic Resonance Imaging (MRI) contrast agents (CAs) has  [,2] since the mid-2000s, when the potentially fatal Nephrogenic Systemic Fibrosis (NSF) was associated with the *in vivo* dechelation of these Gd(III)-based drugs .[3–5] NSF, which causes fibrotic proliferations triggered by gadolinium(III) deposition in the skin and other organs, has been observed mainly in patients with renal faliure.[6,7] As the majority of contrast agents are excreted through kidneys with a half-life of ~1.6 hours, the reduced kidney function results in prolonged residence time in the body, which offers a possibility for the dissociation of Gd(III) complexes through metal or ligand exchange reactions.[8]

In response to the fact that the most NSF cases were observed with open-chain Gd(III) chelates, the complexes of the linear DTPA (diethylenetriaminepentaacetic acid) ligand and its derivatives, their clinical applications have been strictly regulated or prohibited in patients with certain diseases. Obviously, the simplest way to avoid the toxic effect of Gd(III) is to prevent the use of Gd(III)-based CAs. However, contrast enhancement is often required to observe certain lesions and thus reach an accurate diagnosis. However, the replacement of the Gd(III) with other paramagnetic metal ions such as Mn(II) or Fe(III), which are expected to be less toxic than Gd(III) due to their biogenic character, is not a trivial task because of substantial differences in their coordination chemistry.[9–11] Moreover, many research efforts have to be devoted to design and synthesize ligands suitable for the adequate complexation of those metal ions.[2,12] On the other hand, a satisfactory solution to the NSF problem[13,14] can also be provided if the *in vivo* dechelation of the Gd(III) complexes is prevented by increasing the inertness of the chelates.

As it was demonstrated in several studies, rigidification of the chelators can be achieved by incorporating aliphatic or aromatic rings into the ligand skeleton. This provides a rigid coordination cavity with extremely limited internal motion, hindering the dissociation of the Gd(III) complex.[11,15–17] In our recent work we revealed that the phenanthroline backbone incorporated into an aminopolycarboxylate chelate increases significantly the inertness of the Gd(III) chelate, since the [Gd(FENTA)]⁻ complex (FENTA: 1,10-phenanthroline-2,9-diyl)bis(methyliminodiacetic acid, Scheme 1) dissociates 4 times slower than [Gd(DTPA)]⁻, which is still frequently used in clinical practice.[18]

In this work, we report the results of a detailed thermodynamic, kinetic, relaxation, and structural study of the Gd(III) complex of the ligand (2,2',2'',2'''-(([2,2'-bipyridine]-6,6'-diylbis(methylene))bis(azanetriyl))tetraacetic acid). The ligand was firstly synthesized by Mukkala and coworkers[19] for exploiting the luminescence properties of lanthanides, however,

it has not been investigated as a CA candidate so far. The structure of Gd(III) complex was studied by DFT calculations, further aided by luminescence measurements and NMR studies with an aim of rationalizing the obtained physico-chemical data. The results were compared to those obtained for the Gd(III) complexes of ligands , (ethylene glycol-bis(2-aminoethylether)-N,N,N′,N′-tetraacetic acid) and (diethylenetriaminepentaacetic acid). Even though the aromatic N donors of the possess higher basicity than the oxygens of , the position and the number of donor atoms provide an opportunity to compare the coordination chemistry features of the two ligands.[20–22] In addition, studies related to Ln(III) complexation of rigidified derivatives were also reported.[23–26]
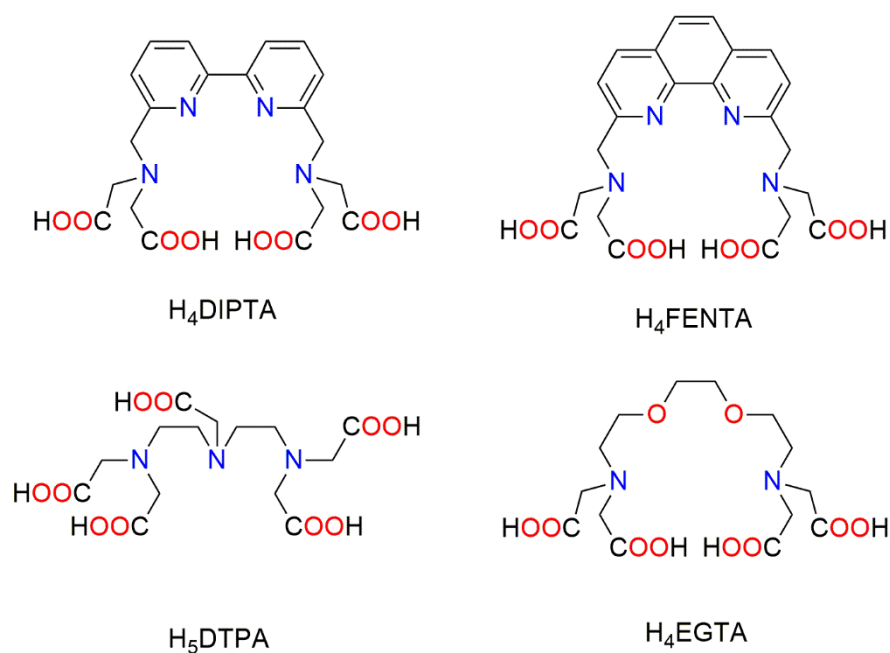


**Scheme 1**. Schematic structure of , , and ligands.

**Results and discussion**

**Synthesis.** The synthesis of the ligand was carried out by the reaction between 6,6′-bis(chloromethyl)-2,2′-bipyridine (CAS: 74065-64-8) and diethyl iminodiacetate (CAS: 6290-05-7) followed by the saponification of the ethyl ester in basic conditions. The ligand was then precipitated from an acidified solution due to the low solubility of the fully protonated ligand.

4

For more details in reference to the synthesis and characterization of the ligand see the ^{1}H, ^{13}C, HMBC and NOESY NMR spectra, the HPLC chromatogram as well as the ESI-MS spectrum provided in the ESI (Figures S1-S9).

**Thermodynamic and kinetic studies.** The protonation constants of the ligand were determined by pH-potentiometric titrations in the presence of NaCl ($I$=0.15 M, at 25 °C) to mimic the physiological electrolytic background. Only three protonation constants could be determined for the ligand, since below pH~4 the ligand precipitated from the solution at the ~2 mM concentration required for these studies. This is most probably due to the low solubility of the neutral form of the ligand . Unfortunately, the same phenomenon was observed for the Gd(III) complex, which does not allow the determination of the stability constant of the complex. However, based on the results gained for the [Gd(FENTA)]$^-$, the same stability for the [Gd(DIPTA)]$^-$ can be envisioned due to the high similarity in their structures. Furthermore, the NMR and relaxometric studies also confirmed the formation of the [Gd(DIPTA)]$^-$ complex.

The PSEQUAD program[27] was used to fit the V(ml)-pH data pairs recorded in the ligand titration. The protonation constants of the were defined by Equation 1 (the square brackets in the equations refer to the equilibrium concentrations of the species).

$$K_i^H = \frac{[H_iL]}{[H^+][H_{i-1}L]} \qquad i=1\text{-}3 \qquad (1)$$

The calculated constants are summarized in Table 1, along with the corresponding values reported for , and ligands. Based on the protonation constant published by Hancock and coworkers for 2,2'-bipyridine ( =4.58, 0.5 M , 25 °C),[28] it can be stated that the first two values of DIPTA$^{4-}$ are related to the protonation of the nitrogen atoms of the iminodiacetic acid moieties (similarly to those of FENTA$^{4-}$). The remaining protonation constant can characterize either the protonation of an aromatic nitrogen atom or an acetate pendant arm.

5

**Table 1**. The protonation constants ( ) of the  ,   and   ligands.[a]

| | | | | |
|---|---|---|---|---|
| | 8.81(6) | 8.30 | 9.43 | 9.93 |
| | 8.43(4) | 7.41 | 8.82 | 8.37 |
| | 4.01(6) | 3.52 | 2.77 | 4.18 |
| | – | 2.98 | 2.06 | 2.71 |
| | – | 2.07 | 1.88 | 2.00 |
| $\Sigma^{,2}$ | *17.24* | *15.71* | *18.25* | *18.30* |

[a] $3\sigma$ standard deviations are indicated in parenthesis. $I = 0.15$ M NaCl, T = 298 K. [b] Ref.[18], [c] Ref.[20], [d] Ref.[29]

The basicity of different ligands is frequently compared by the sum of the   values characterizing the basicity of the amine N atoms of the ligand backbone, since these protonations have essential impact on the complex formation. Therefore, only the first two   of the ligands ($\Sigma^{,2}$) were considered in the calculations. Based on this value, the basicity of the ligand backbone of DIPTA$^{4-}$ is close to that of FENTA$^{4-}$. However, $\Sigma^{,2}$ of the two aliphatic ligands EGTA$^{4-}$ and DTPA$^{5-}$ are ca. 2 orders of magnitude higher than that of DIPTA$^{4-}$. Interestingly, the lack of the central aromatic part of the phenanthroline unit does not affect significantly the basicity of the ligand, but has a dramatic effect on the kinetics of dissociation of the Gd(III) complex (*vide infra*).

In order to characterize the decomplexation of [Gd(DIPTA)]$^{-}$, metal exchange reactions were carried out with 20-fold excess of Lu(III) used as a scavenger for the ligand (under these conditions the displacement is 100%). The exchange reactions were followed by $^1$H relaxometry in the pH range between 3.3 to 5.5 (precipitation was not observed in the investigated pH range). The high excess of the Lu(III) ion ensures pseudo-first order conditions,

thus the values obtained are pseudo-first order rate constants and expressed as follows (Equation 2):

$$-\frac{d[Gd(DIPTA)^-]_t}{dt}=k_{obs}[Gd(DIPTA)]_t \tag{2}$$

where $[Gd(DIPTA)]_t$ is the total concentration of the complex.

The Ln(III) complexes of polyamino polycarboxylate ligands mainly dissociate through proton-assisted pathways but in certain cases the spontaneous dechelation and/or the metal-assisted routes can also operate. For the efficient attack of an exchanging metal ion on the chelate, a dinuclear intermediate with sufficiently high stability must be formed, as it was previously described also for the Gd(III) complex of the linear $DTPA^{5-}$ ligand.[30] In order to explore the impact of this pathway on the rate of dissociation for $[Gd(DIPTA)]^-$, exchange reactions were also carried out in the presence of 40-fold excess of Lu(III) at 3 different pH values (Figure 1).
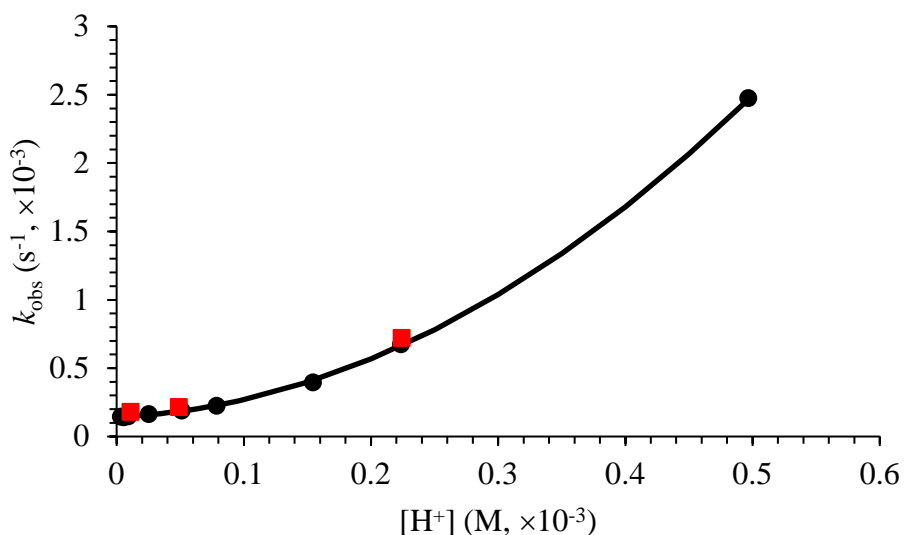
**Figure 1**. Dependence of the pseudo-first-order rate constants ( ) on [H$^+$] for the [Gd(DIPTA)]$^-$ complex at 20- (●) and 40-fold (■) excess of Lu(III). The lines correspond to the best fit of the values.

As it is highlighted in Figure 1, the values recorded at different initial Lu(III) concentration do not differ within the experimental error limits. The rate constants increase by increasing the H$^+$ concentration with a non-negligible intercept on the y-axis indicating the presence of the spontaneous dissociation pathway in the exchange reactions. Furthermore, the values have a second-order dependence on [H$^+$], which can be defined as follows (Equation 3):

$$= \ + \ [H^+] + \ [H^+]^2 \tag{3}$$

The rate constants of the different pathways are presented in Table 2, where the corresponding values determined for complexes [Gd(FENTA)]$^-$, [Gd(EGTA)]$^-$ and [Gd(DTPA)]$^{2-}$ are also shown.

**Table 2**. Rate constants for the dissociation reactions of [Gd(DIPTA)]$^-$, [Gd(FENTA)]$^-$, [Gd(EGTA)]$^-$ and [Gd(DTPA)]$^{2-}$and their half-lives calculated at pH=7.4 (25 °C)

| | [Gd(DIPTA)]$^-$ | [Gd(FENTA)]$^{-a}$ | [Gd(EGTA)]$^{-b}$ | [Gd(DTPA)]$^{2-c}$ |
|---|---|---|---|---|
| (s$^{-1}$) | (1.44±0.08)×10$^{-4}$ | – | – | – |
| (M$^{-1}$s$^{-1}$) | 0.40(8) | 0.23 | 60 | 0.58 |
| (M$^{-2}$s$^{-1}$) | (8.6±0.4)×10$^3$ | 250 | – | 9.7×10$^4$ |
| $_{/2}$ (days)$^d$ | 0.06 (1.34 h) | 872 | 3.4 | 202 |

[a] Ref.[18]; [b]Ref.[23], [c] Ref.[30]; [d] $_{/2}$=ln2/ , pH=7.4

By analyzing the results, it is clear that the proton-assisted dissociation of [Gd(DIPTA)]$^-$ occurs slower than that of the [Gd(DTPA)]$^-$, while it is somewhat faster than that observed for [Gd(FENTA)]$^-$. Obviously, the incorporation of the bypiridine moiety into the ligand backbone provides a more rigid coordination cavity for the DIPTA$^{4-}$ complex than for the DTPA$^{5-}$ analogue, but its rigidity is lower than that of FENTA$^{4-}$. Furthermore, the free rotation of the two pyridine moieties around the bond at positions 6,6', seemingly divides the structure of the ligand in two parts, which could facilitate the simultaneous decoordination of the donor atoms leading to spontaneous dissociation. For a better comparison of the inertness of the three chelates, the half-lives ($_{/2}$) of their dissociation reactions were calculated for physiological pH (Table 2). Unfortunately, the presence of the spontaneous dissociation in the dechelation process of [Gd(DIPTA)]$^-$ decreases its inertness more than 3 orders of magnitude compared to the FENTA$^{4-}$ and DTPA$^{5-}$ complexes, while it is dissociating 56 times faster than [Gd(EGTA)]$^-$, which is obviously unfavorable for the *in vivo* application.
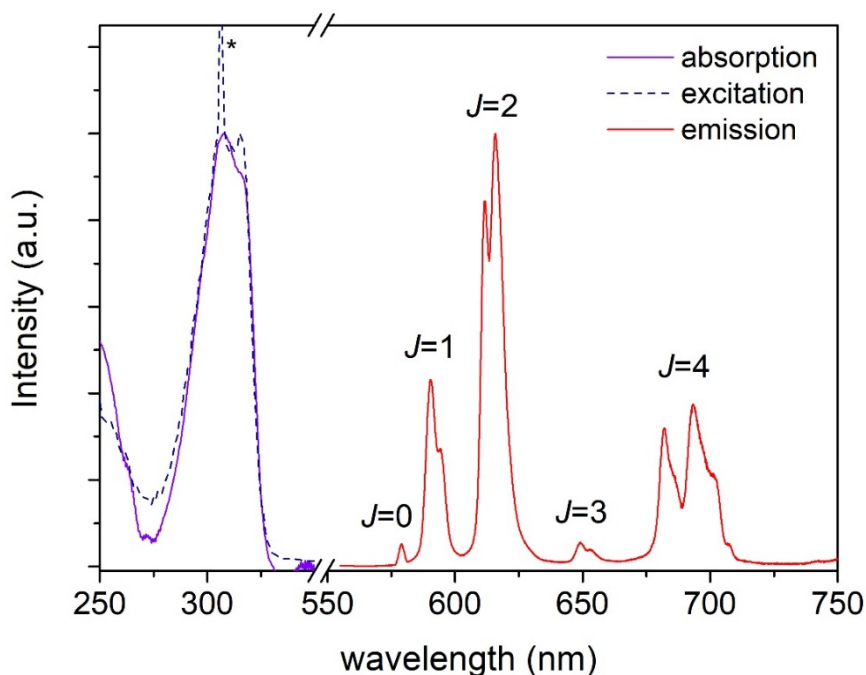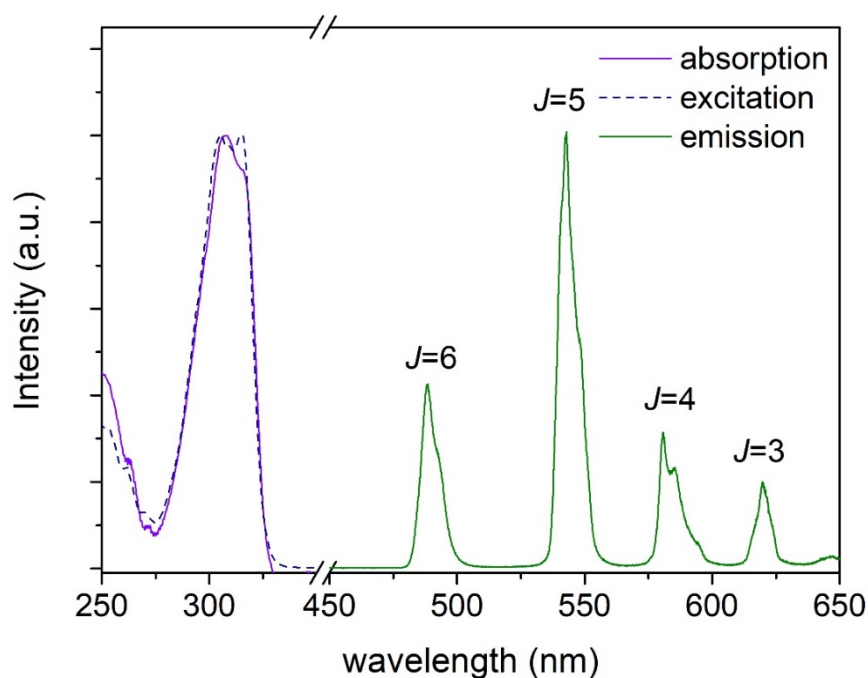
**Figure 2.** Excitation, absorption and emission spectra recorded for $10^{-5}$ M solutions of [Eu(DIPTA)]$^-$ (top, $\lambda_{ex} = 318$ nm, $\lambda_{em} = 613$ nm) and [Tb(DIPTA)]$^-$ (bottom, $\lambda_{ex} = 315$ nm, $\lambda_{em} = 545$ nm) at pH = 7.4 (0.1 M Tris buffer).

**Photophysical properties.** The emission spectra of the [Eu(DIPTA)]$^-$ and [Tb(DIPTA)]$^-$ complexes were recorded in buffered aqueous solutions (pH 7.4, Tris buffer) under excitation through the ligand bands at ~315 nm. The emission spectra display the characteristic $\rightarrow$ ($J = 0 - 4$) and $\rightarrow$ ($J = 6 - 3$) transitions of Eu(III) and Tb(III), respectively (Figure 2).[31] In both cases the absorption and excitation spectra are virtually superimposable, confirming indirect excitation of the metal ion by energy transfer from ligand-centered excited states. The absorption spectra display maxima at 300 nm typical of the bipyridil chromophore.[32–34] The emission of the [Eu(DIPTA)]$^-$ complex is dominated by the $\rightarrow$ transition. This, together with the sizeable intensity of the $\rightarrow$ transition, suggests a low symmetry of the crystal field generated by the coordination of the ligand to the metal ion.[35]

The lifetimes of the excited and levels of Eu(III) and Tb(III) were mesured in and solutions to estimate the number of water molecules coordinated to the metal ion using the method proposed by Horrocks[36] and refined by Beeby.[37] The emission decays are monoexponential, affording lifetimes of $\tau_{H_2O}$ = 0.598 and $\tau_{D_2O}$ = 2.17 ms for Eu(III) and $\tau_{H_2O}$ = 1.03 and $\tau_{D_2O}$ = 1.46 ms for Tb(III) (Figures S11-S12, ESI). The lifetime in measured for [Eu(DIPTA)]$^-$ is very similar to that reported by Mukkala,[19] and is typical of Eu(III) complexes containing a coordinated water molecule. However, the $\tau_{H_2O}$ value reported for [Tb(DIPTA)]$^-$ by Mukkala (1.22 ms) is somewhat longer than the value determined in this study. The emission lifetimes afford $q$ values of 1.0 and 1.15 for the Eu(III) complex using the expressions proposed by Horrocks[36,38] and Beeby,[37] respectively. For the Tb(III) analogue, the expression proposed by Beeby yields $q$= 1.15. Thus, these studies unambiguously confirm the presence of a water molecule coordinated to the Ln(III) ion in aqueous solution. The emission quantum yields determined for [Eu(DIPTA)]$^-$ ($\Phi$ = 8%) and [Tb(DIPTA)]$^-$ ($\Phi$ = 35%) are similar to those determined previously for the FENTA analogues.

## $^1$H and $^{13}$C NMR studies.

The complex formation of DIPTA with Gd(III) was further confirmed by NMR studies, using the Eu(III) and Lu(III) DIPTA$^{4-}$ analogues. The $^1$H NMR spectra of [Eu(DIPTA)]$^-$ and [Lu(DIPTA)]$^-$ are shown in Figure 3, where they are compared with that of the free ligand. It is clearly visible that in the case of Lu(III) the $^1$H signals of the aliphatic protons (3-4.5 ppm) are broadened, and the signal of the iminodiacetate pendants are somewhat split. These changes in the spectrum reveal that the amino-carboxylate pendants take part in the complex formation, as confirmed by the extremely broad aliphatic proton signals (2-4.5 ppm) in the spectrum of [Eu(DIPTA)]$^-$. Here the paramagnetism of Eu(III) results in the paramagnetic shift of all signals (Figure 3, S6 and S10), more notably that of the aromatic protons closest to the amino-

carboxylate pendants (See the ESI for more details). We note that the ^{1}H NMR signals observed for the Eu(III) complex experience small paramagnetic shifts, a situation that was observed previously for certain non-macrocyclic Eu(III) complexes, and was related to a small magnetic anisotropy resulting in small pseudocontact shifts.[39]Small paramagnetic shifts in fluxional Ln(III) complexes were also attributed to different conformations present in solution in fast exchange.[40]

Variable temperature NMR experiments evidence remarkable changes in the NMR signals of aliphatic protons of both the Eu(III) and Lu(III) complexes, in the temperature range 283-308 K (Figure S6, ESI). The changes in the linewidths of these resonances reflect dynamic interconversion processes taking place in solution, which can be ascribed to the interconversions between the in-plane and out-of-plane acetate groups, as demonstrated previously for structurally related complexes.[20,41]
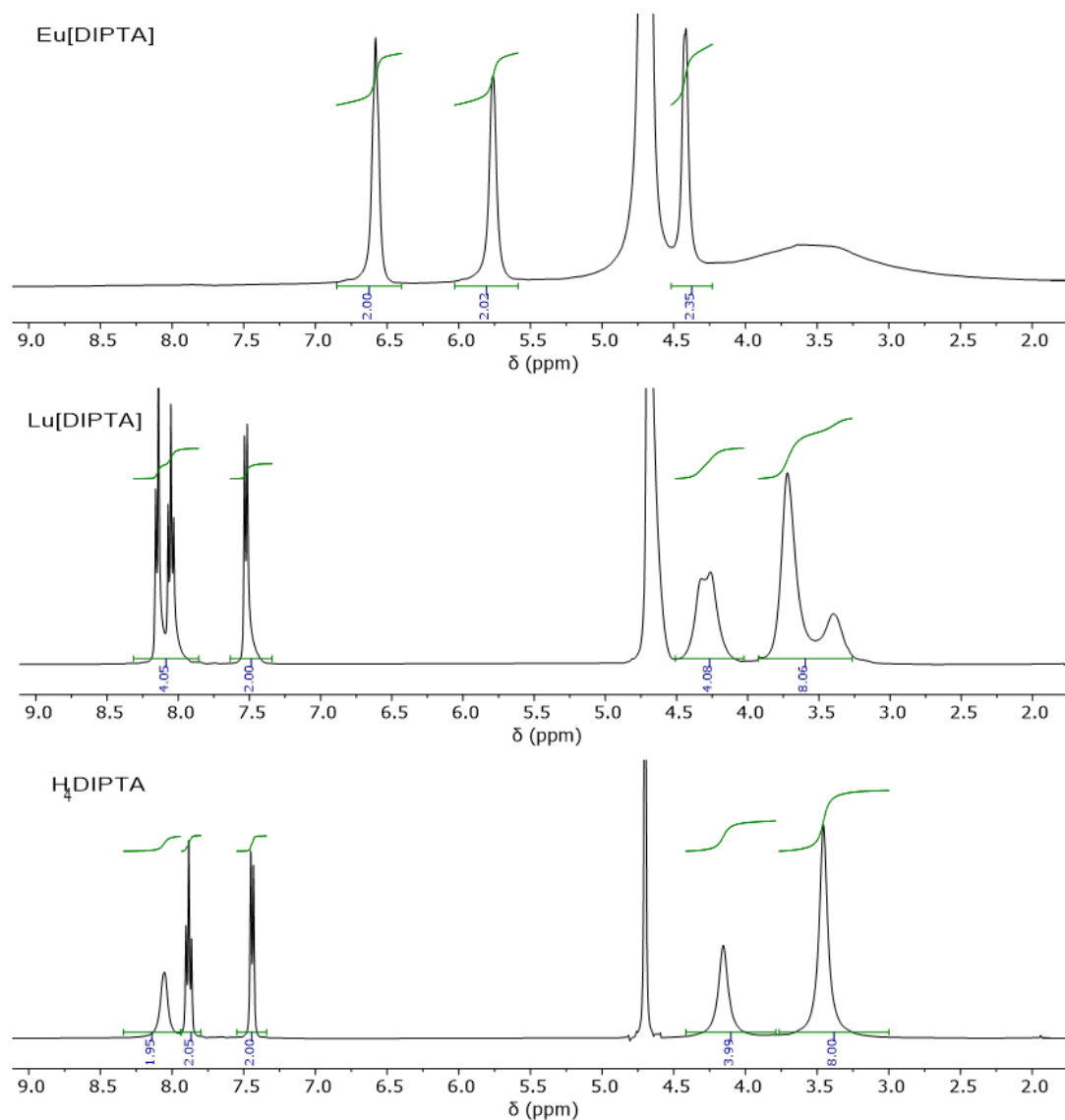
**Figure 3**. ^{1}H NMR spectra of the ligand (pH = 9.2), [Lu(DIPTA)]− (pH = 10) and [Eu(DIPTA)]− (pH = 6.5) complexes ( , T=298 K).

The self-diffusion coefficients were measured for the ligand and both complexes at 298 K. In the case of [Eu(DIPTA)]− only the aromatic proton signals could be used for the determination of the diffusion coefficient. The diffusion coefficient of the ligand was found to be $D = 3.5 \times 10^{-10}$ m$^2$/s, while values of $4.11 \times 10^{-10}$ m$^2$/s and $3.92 \times 10^{-10}$ m$^2$/s were obtained for [Lu(DIPTA)]− and [Eu(DIPTA)]−, respectively. The higher $D$ values determined for the

complexes are related to their smaller hydrodynamic size as the ligand wraps around the metal ion.

**DFT calculations.** The structure of the [Gd(DIPTA)]⁻ complex was calculated by using DFT methods. The calculations utilized two explicit second-sphere water molecules, while the effect of bulk solvent water molecules was considered by the use of the polarized continuum model (PCM). This approach provided a high degree of accuracy in the prediction of Gd- distances, and the spin density localized at the O nuclei of the water molecule.[18,42,43] Moreover, the dispersion corrections were added to our DFT calculations for a more accurate prediction of inter- and intramolecular interactions. Details are provided in the Experimental section.

The calculated structure of the [Gd(DIPTA)]⁻ complex is shown in Figure 4 and the corresponding Cartesian coordinates are available in the SI (Table S1).
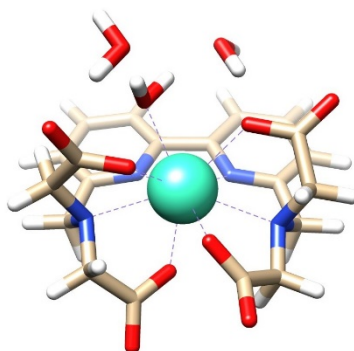


**Figure 4**. Calculated structure of [Gd(DIPTA)]⁻ complex.

DFT calculations provided a distorted tricapped trigonal prism coordination polyhedron for Gd(III). The ligand binds the metal ion with (4O,4N) donor sets and the coordinated water molecules complete the coordination sphere of Gd(III). This water molecule is stabilized by the explicit water molecules through a strong hydrogen-bond network. Moreover, the acetate pendant arms further stabilize these water molecules. The calculated bond lengths between Gd(III) and nitrogen donor atoms or coordinated water molecule are similar to those obtained for the [Gd(FENTA)]⁻ complex (Table 3.)

**Table 3**. Calculated bond distances of the [Gd(DIPTA)]⁻ and [Gd(FENTA)]⁻ complexes.

| Distance (Å) | Gd(III) – | Gd(III) – | Gd(III) – | Gd(III) – | Gd(III) – |
|---|---|---|---|---|---|
| [Gd(DIPTA)]⁻ | 2.65 | 2.66 | 2.67 | 2.69 | 2.55 |
| [Gd(FENTA)]⁻ ᵃ | 2.64 | 2.67 | 2.67 | 2.73 | 2.45 |

ᵃ Data are taken from Ref.[18]

The calculated bond lengths and angles are very similar for the two complexes, thus, it is reasonable to assume that the two complexes possess similar stability. However, the calculated bond length between Gd(III) and the water molecule is longer for [Gd(DIPTA)]⁻ than that of [Gd(FENTA)]⁻ complex. Since this distance falls into the range of first coordination sphere, we expect somewhat lower relaxivity for the [Gd(DIPTA)]⁻ complex. This assumption is confirmed experimentally in the subsequent part of the paper.

**Relaxivity and ¹⁷O NMR measurements.** Since the rate of the relaxation enhancement effect is a key parameter of MRI CA candidates, the longitudinal ( ) water proton relaxivities were determined for [Gd(DIPTA)]⁻ using ¹H relaxometry at magnetic field strengths of 0.49 and 1.41 T. To maintain the physiologically relevant pH, HEPES buffer was used in 50 mM concentration ( = 7.4, $I = 0.15$ M NaCl). The measurements were carried out either at 25 and 37 °C and at 3 different concentrations of the complex. The recorded relaxation rates (1/ ) were then plotted versus the Gd(III) concentrations and the  values were evaluated (data are shown in ESI, Figures S13 and S14). The results are presented in Table 4 along with the  values determined for [Gd(FENTA)]⁻ and [Gd(DTPA)]²⁻. Furthermore, to get better insight into the *in*

*vivo* relaxivity of the complex, the values were also measured in human serum for [Gd(DIPTA)]⁻ at both field strengths (37 °C).

**Table 4**. The values ($mM^{-1}s^{-1}$) determined for the Gd(III) complexes of $DIPTA^{4-}$, $FENTA^{4-}$ and $DTPA^{5-}$ ligands at pH=7.4 and 25/37 °C.

| | | [Gd(DIPTA)]⁻ | [Gd(FENTA)]⁻[a] | [Gd(DTPA)]²⁻ |
|---|---|---|---|---|
| 0.47 T | 25 °C | 5.06 | 5.56 | 4.69[b] |
| | 37 °C | 4.98 | 4.42 | 3.8[c] |
| | 37 °C plasma/serum | 6.12[d] | 7.79[d] | 3.8[e] |
| 1.41 T | 25 °C | 4.96 | 5.36 | 4.24[b,f] |
| | 37 °C | 3.71 | 4.03 | 3.4[c] |
| | 37 °C plasma/serum | 5.62[d] | 6.95[d] | 4.1[e] |

[a] Ref.[18], [b] Ref.[44]; [c] Ref.[45]; [d] SeronormTM (serum), [e] Ref.[46] (plasma), [f] 50 MHz = 1.17 T,

The relaxivity values of [Gd(DIPTA)]⁻ are generally lower than those found for [Gd(FENTA)]⁻ at both magnetic field strengths and temperatures studied, but slightly higher than those of [Gd(DTPA)]²⁻. The only exception arises from the value measured at 37 ºC, which is higher for [Gd(DIPTA)]⁻ than for [Gd(FENTA)]⁻ (Table 1) Furthermore, the value measured at 0.47 T 37 ºC is only slightly lower than that recorded at 25 ºC. A detailed investigation of the relaxivity at variable magnetic fields would be required to assess the origin of this unusual feature. The relaxivity values decrease with increasing of temperature at both magnetic fields (at 20 MHz a slight decrease was observed), indicating that the relaxivity is controlled by fast rotation of the complex, which is typical for low molecular weight Gd(III) complexes.[47] The 10-20% increase in the relaxivity values measured in the presence of human

serum indicates a small increase of the rotational-correlation time ($\tau_R$) related to the formation of low stability adduct, which improves slightly the relaxation enhancement effect.

The combination of the effect of numerous microscopic parameters regulates the relaxivity of the Gd(III) complexes. One of the most important factors is the exchange rate of the inner sphere water molecule, , which ensures the "transfer" of the paramagnetic effect to the bulk water. In order to obtain information on the water exchange rate of [Gd(DIPTA)]⁻, variable temperature $^{17}O$ NMR measurements were performed (at 400 MHz, 9.4 T). For the calculation of the rate of water exchange, the reduced transverse $^{17}O$ relaxation rates (1/ ) as well as chemical shifts ($\Delta\omega_r$) were recorded, and the hyperfine coupling constant ($A/\hbar$) and the electronic longitudinal relaxation rates (1/ ) were used as fitting parameters according to the Swift-Connick theory (more details in the ESI), assuming a simple exponential behavior with temperature for electron spin relaxation.[48,49] The activation energy of the electron spin relaxation was set to 1 kJ/mol, furthermore based on the value (5.06 mM⁻¹s⁻¹) and the $q$ values determined by luminescence measurements, the number of coordinated water molecules was set to 1. The temperature dependence of 1/ basically depends on two factors,[50] the transverse relaxation time of the bound water molecule ( ) and the mean residence time of that water molecule ($\tau_m$) in the inner sphere of the complex (1/ ~1/( +$\tau_m$)). Given that increases, while $\tau_m$ decreases with increasing temperature, it is obvious that the 1/ values of [Gd(DIPTA)]⁻ are in the fast water exchange regime (Figure 5), where $\gg \tau_m$.

Since water exchange is fast for [Gd(DIPTA)]⁻, the 1/ values increase steadily without reaching a maximum at low temperatures, the fitting procedure did not deliver acceptable results when , $\Delta H^{\ddagger}$, $A/\hbar$ and 1/ were fitted simultaneously. In order to get acceptable results, the activation enthalpy of the water exchange was set to 29.3 kJ/mol, the value which was determined for the [Gd(FENTA)]⁻ complex. Based on the similar structure of the two ligands, this assumption appears to be reasonable. The parameters afforded by the fitting procedure are

17

listed in Table 5 along with the corresponding values determined for the [Gd(FENTA)]$^-$ and

[Gd(DTPA)]$^{2-}$. The contribution of the water exchange to the overall correlation time $(1/ = +1/)$

was calculated and found to be increasing from 46 to 95% in the temperature range 273-348 K,

which ensures an accurate determination of .

The value of obtained for [Gd(DIPTA)]$^-$ is higher by circa 30% than those were

determined for [Gd(FENTA)]$^-$ and [Gd(EGTA)]$^-$ but more than an order of magnitude higher

than that was obtained for [Gd(DTPA)]$^{2-}$.[51] Interestingly, the electronic relaxation and the

hyperfine coupling constant characterizing the hyperfine interaction between the electron spin

of the Gd(III) and the spin of the $^{17}$O nucleus of water molecule, are almost identical for the

DIPTA and FENTA complexes, which can be explained by the similar structure of the two

chelates. However, the slight increase of the exchange rate can be the result of a higher steric

compression around the water binding site, as it was reported for the [Gd(DOTA)]$^-$ and

[Gd(DODPA)]$^+$ complexes.[52–54] The longer Gd- distance calculated for [Gd(DIPTA)]$^-$

compared with [Gd(FENTA)]$^-$ supports this hypothesis, as a weak Gd- interactions is expected

to facilitate water exchange following a dissociative mechanism.
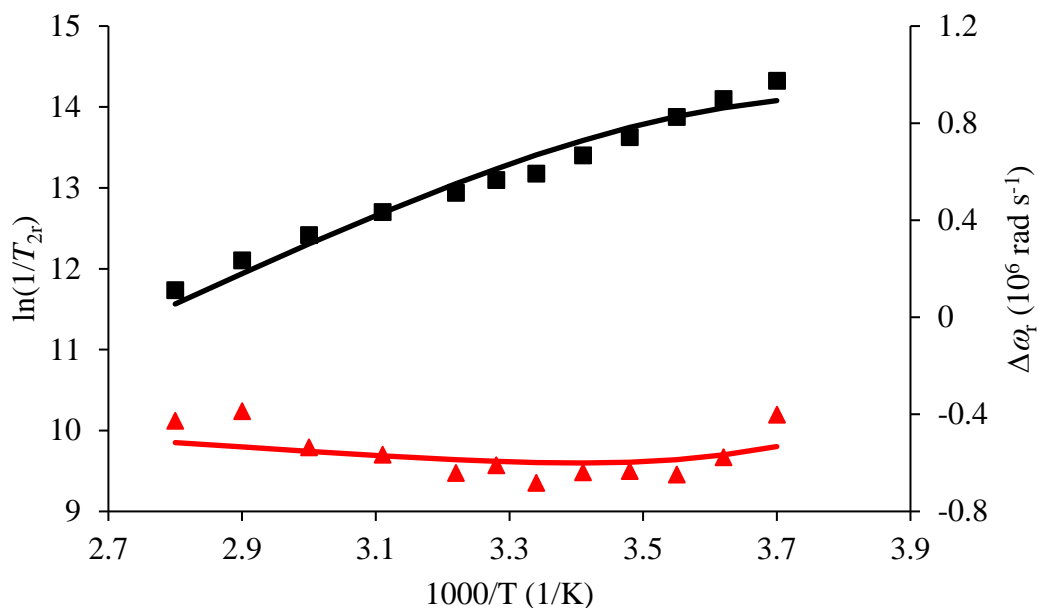
**Figure 5**. Reduced transverse [17]O relaxation rates (■) and [17]O chemical shifts (▲) observed for [Gd(FENTA)][−] solution at 9.4 T and pH=7.4 ( =19.84 mM).

**Table 5**. Best-fit parameters obtained from the analysis of the reduced relaxation ^{17}O NMR rates of [Gd(DIPTA)][−] recorded at 9.4 T together with the corresponding values of [Gd(FENTA)][−] and [Gd(DTPA)][2−].

| | [Gd(DIPTA)][−] | [Gd(FENTA)][−b] | [Gd(EGTA)][−c] | [Gd(DTPA)][2−d] |
|---|---|---|---|---|
| / $10^6$ s$^{-1}$ | 43(5) | 29 | 31 | 3.3 |
| $\Delta H^{\ddagger}$ / kJ mol$^{-1}$ | $29^a$ | 29 | 11 | 51.6 |
| $A/\hbar$ / $10^6$ rad s$^{-1}$ | -2.8(2) | -2.77 | -3.2 | -3.8 |
| 1/ / $10^7$ s$^{-1}$ | 1.5(3) | 1.5 | – | – |

[a] fixed during the fitting procedure, [b] Ref.[18], [c] Ref.[22], [d] Ref.[44]

The hyperfine coupling constant ($A/\hbar$ = −2.8(2)×$10^6$ rad s$^{-1}$) of [Gd(DIPTA)][−] is much lower than the average value reported for Gd(III) complexes (−3.9±0.3×$10^6$ rad s$^{-1}$),[55] which could indicate the lower value of *q*. Nonetheless, the high relaxivity found for [Gd(DIPTA)][−], =5.06

mM$^{-1}$s$^{-1}$ at 0.47 T and 25 °C, suggests the opposite. The good agreement between the estimated and DFT calculated hyperfine coupling constant ($A/\hbar = -2.6 \times 10^6$ rad s$^{-1}$) further corroborates the presence of a coordinated water molecule. Furthermore, similarly low $A/\hbar$ values were reported for the [Gd(OCTAPA)]$^-$ (-2.31×10$^6$ rad s$^{-1}$),[14] [Gd(CHXOCTAPA)]$^-$ (-3.06×10$^6$ rad s$^{-1}$)[72] and [Gd(DODPA)]$^+$ (-2.2×10$^6$ rad s$^{-1}$)[16] complexes, which contain aromatic groups in their structures. This phenomenon suggests that the aromatic moieties may have an effect on the hyperfine coupling constants, probably due to the efficient delocalization of spin density.

**Conclusions**

In this work, the physico-chemical properties of a 2,2'-bipyridine-based acyclic DIPTA ligand and its lanthanide complexes have been studied in detail. Unfortunately, the determination of the thermodynamic stability of the Gd(III) complex was hindered by the low solubility of the protonated Gd(III) complex in acidic condition. However, based on the results obtained for the structurally similar [Gd(FENTA)]$^-$, comparable stability with that of [Gd(DIPTA)]$^-$ is assumed. Interestingly, the inertness of [Gd(DIPTA)]$^-$, despite its more rigid structure, is lower than that was observed for the [Gd(EGTA)]$^-$, which phenomenon can be explained by the appearance of the spontaneous dissociation pathway in the dechelation of that. The relaxation enhancement effect determined for [Gd(DIPTA)]$^-$ does not differ significantly from that of [Gd(FENTA)]$^-$ but somewhat higher than that of [Gd(DTPA)]$^{2-}$ complex. The [Gd(DIPTA)]$^-$ possesses higher exchange rate for the inner sphere water molecule than [Gd(FENTA)]$^-$ complex due to the more flexible structure of the ligand. DFT calculations suggested a distorted tricapped trigonal prism polyhedron for the Gd(III) chelate with one inner sphere water molecule ($q$=1) which result was confirmed by the luminescence emission lifetime measurements carried out with the [Eu(DIPTA)]$^-$ and [Tb(DIPTA)]$^-$ complexes. Overall, we can conclude that the replacement of the phenantroline with bipyridine unit in the ligand backbone does not have large effect on the thermodynamic and relaxation properties of the Gd(III) complex, yet the inertness decreases by

orders of magnitude which is unfavourable for the *in vivo* application of the complexes. Thus, we propose the incorporation of phenanthroline backbone instead of bipyridine in further design of platform of CAs.

**Experimental section**

The ligand was synthetized in our laboratory, while the other materials used in the different experiments were purchased from commercial sources and used without further purification (the purity of salt is 99.9%). The concentration of the solutions was determined with known concentrated solution (0.01 M) in the presence of xylenol orange as indicator. The [Ln(DIPTA)]⁻ complexes were prepared by mixing the solution of the ligand and Ln(III) ion of known concentrations to reach 1:1 stoichiometric ratio, followed by pH adjustment.

**Equilibrium studies.** The protonation constant of the ligand were determined by pH-potentiometric titrations. The concentration of the ligand stock solution was calculated from the titration curves. For the pH-potentiometric titrations, a Metrohm 888 Titrando titration workstation and a Metrohm-6.0233.100 combined electrode were used. KH-phthalate (pH=4.005) and borax (pH=9.177) buffers were used to calibrate the electrode. To avoid the effect of the titrations were carried out under inert atmosphere( ) in 6.0 mL samples at 25 °C. The samples were stirred during the titration. 0.15 M NaCl ionic strength was used to mimic the in vivo circumstances. 0.2 M NaOH was used to titrate the samples containing the ligand in 2 mM concentration. 150-200 mL–pH data pairs were recorded in the pH range of 1.8-12.0. In order to characterize the electrode answer for the pH change, the Irving factor was determined in a HCl-NaOH titration, from which the ion product of water ( ) was also calculated.[56] The equilibrium constants were evaluated by using the PSEQUAD program.[27]

**Kinetic measurements.** The rate of the exchange reactions between the [Gd(DIPTA)]$^-$ and the Lu(III) was investigated at 25 °C and 0.15 M NaCl ionic strength by a Bruker Minispec MQ-60 NMR Analyzer measuring the 1/ relaxation rates. The reactions were carried out in the pH range between 3.3 – 5.5. The concentration of [Gd(DIPTA)]$^-$ was 1 mM while 20-fold excess of Lu(III) was applied. The pH was maintained by a mixture of non-coordinating buffers, 1-methylpiperazine ( =4.9, 50 mM) and 1,4-dimethylpiperazine ( =4.2, 50 mM). In order to exclude the presence of the metal-assisted dissociation pathway, the rate of the dissociation was also studied with 40-fold excess of Lu(III) at 3 different pH values. The high excess of exchanging metal ion ensures the pseudo-first order conditions. The fitting of the data was carried out with the program Micromath Scientist (Salt Lake City, UT, USA) using a least-squares fitting approach. The pseudo-first-order rate constants ( ) were obtained by fitting the 1/ values measured at different times on the basis of Equation 4.

$$R_t = (R_0 - R_e)e^{-k_{obs}t} + R_e \tag{4}$$

where , , and   are the relaxivity values measured at the start, at time t, and at equilibrium, respectively.

**Luminescence measurements.** Absorption UV−vis spectra were recorded on a JENWAY 6850 UV−vis spectrometer with 4 mm quartz cells. Steady-state excitation and emission spectra were recorded with a Horiba FluoroMax Plus-P spectrofluorometer equipped with a continuous 150 W xenon arc lamp (ozone-free), an R928P photon counting emission detector, and a photodiode reference detector for monitoring lamp output. Luminescence lifetimes were determined with the time-correlated single-photon counting method using a xenon flash lamp. Quantum yields were measured using the Eu(III) and Tb(III) tris-picolinates

as standards.[57,58] The errors in emission lifetimes are estimated to be $\pm$ 10% and in quantum yields $\pm$ 15%.

**DFT calculations.** Ground state geometry of the Gd(III) complex was computed through the Gaussian 16 software package (AM64L-G16 RevB.01) at the DFT level of theory.[59] The calculations utilized the DFT dispersion correction with Becke–Johnson damping (DFT-D3(BJ))[60] to accurately describe the inter- and intramolecular interactions. The TPSSh[61,62] exchange-correlation functional was used with the quasi-relativistic effective core potential including 53 electrons in the core (ECP53MWB) with the corresponding (7s6p5d)/[5s4p3d] basis sets for Gd.[63,64] All other atoms (C, H, N, O) were treated with the 6-311G(d,p) basis set. The effect of the solvent was taken into account by the polarizable continuum model (PCM).[65] Single-point frequency calculations were also carried out for the ground state geometry at the same level of theory, which represented a true energy minimum on the potential energy surface.

$^{17}$O hyperfine coupling constant was computed through the ORCA software (version 5.0.3)[66] with the TPSSh functional. In this calculation, the atom-pairwise dispersion correction with the Becke-Johnson damping scheme (D3BJ) was utilized. The SARC2-DKH-QZVP[67] basis set was used for Gd, while the other atoms were treated with the DKH-def2-TZVP according to the protocol reported earlier.[68,69] The resolution of identity and chain of spheres exchange (RIJCOSX) approximation was used to accelerate the calculations with the SARC2-DKH-QZVP/JK auxiliary basis set for Gd, while the auxiliary basis set of the other atoms were generated through the AutoAux procedure.[70–72] The calculation included the polarizable continuum model to consider the effect of the solvent. In these calculations, tight SCF convergence criteria were employed.

**Relaxivity measurements.** The $^{1}$H longitudinal relaxation times were measured by using Bruker Minispec MQ 20 and MQ-60 NMR Analyzers (0.47 and 1.41 T) at 25.0($\pm$0.2) or

37.0(±0.2) °C. Inversion−recovery method (180°−τ−90°) was used to determine    values averaging 4−6 data points obtained at 10 different τ delay values. The relaxivity values were obtained from the slopes of plots 1/  versus  $_{(III)}$ for 3 concentrations. HEPES buffer (0.05 M) was used to maintain the pH (7.4) of the samples. The   values of the [Gd(DIPTA)]⁻ in human serum were determined by using Seronorm solution (SeronormTM SERO = lyophilized human blood serum with no preservatives or stabilizers added). One bottle of lyophilized serum was dissolved in 4 ml of water. After the complete dissolution, 1 ml of a 5.0 mM complex solution was added and pH was adjusted to 7.4.

**¹⁷O NMR measurement.** The longitudinal ( ) and transverse ( ) relaxation times of the ¹⁷O nuclei and its chemical shifts were measured on an aqueous solution of the Gd(III) complex (pH = 7.4, at 19.84 mM concentration) and on a diamagnetic reference ( acidified water, pH = 3.3) in the temperature range 273–348 K using a Bruker Avance 400 (9.4 T, 54.2 MHz) spectrometer. The temperature was determined according to well-established calibration routines using ethylene glycol as standard.[73]   and   values were determined by the inversion−recovery and the CPMG techniques, respectively.[74,75] To avoid susceptibility corrections of the chemical shifts, a glass sphere fitted into a 10 mm NMR tube was used during the measurements. To increase the sensitivity of ¹⁷O NMR measurements, ¹⁷O enriched water (10% , NUKEM) was added to the solutions to reach a 2% enrichment. The data fit was carried out with the program Micromath Scientist using least squares fitting procedure. The ln(1/ ) and $\omega_r$ values were fitted to the Swift-Connick equations[48,49] assuming simple exponential behavior of the electron spin relaxation (Figure 5). The   values showed negligible difference between the Gd(III) complex and the reference, thus were not included in the calculations.

**NMR measurements**. ¹H, ¹³C, NOESY (nuclear overhauser enhancement spectroscopy), HMBC (heteronuclear multiple bond correlation) and DOSY (diffusion-ordered spectroscopy) NMR experiments were performed with a 360 Bruker Avance I NMR

spectrometer and a 400 MHz Bruker Avance II instrument equipped with a gradient probe head, at 298 K, using the standard pulse sequences. The samples were dissolved in  (VWR, 99.96% D). The mixing time for the NOESY experiment was set to 1 s. Diffusion properties of the ligand and the Eu[DIPTA] and Lu[DIPTA] complexes were determined with pulse gradient spin echo (PGSE) pulse sequence using bipolar gradient pulses (BIPLED). To reach the proper exponential intensity decrease, the diffusion time ($\Delta$) was set between 30-50 ms, while the gradient pulse length ($\delta$) was changed between 4-6 ms. The gradient strength ($G$) was increased in 32-64 square distant steps. MestReNova 9.0 was used for processing the spectra. Diffusion coefficients ( ) were calculated according to Equation 5.[76]

$$I = I_0 \, exp(- D_{obs}\gamma^2\delta^2 G^2(\Delta - \delta/3)) \tag{5}$$

where $I$ and   are the measured and initial signal integrals respectively, $\gamma$ is the gyromagnetic ration of $^1$H nuclei. The exponential curves were fitted by the nonlinear least-squares method, while the obtained diffusion coefficients were calibrated for HDO in  .[77]

ASSOCIATED CONTENT

**Electronic Supplementary Information**. Details on the synthesis, $^1$H, $^{13}$C, HMBC, NOESY and COSY NMR and MS spectra of the ligand, UV-vis absorption spectra, luminescence measurements, energy and Cartesian coordinates obtained by DFT, relaxometric and NMR studies.

AUTHOR INFORMATION

**Corresponding Author**

E-mail for Ferenc K. Kálmán: kalman.ferenc@science.unideb.hu

## Author Contributions

The manuscript was written through contributions of all authors. All authors have given approval to the final version of the manuscript.

## Notes

The authors declare no competing financial interest and there are no conflicts to declare.

REFERENCES

1  G. Tircsó, E. Molnár, T. Csupász, Z. Garda, R. Botár, F. K. Kálmán, Z. Kovács, E. Brücher and I. Tóth, in *Metal Ions in Bio-Imaging Techniques*, eds. A. Sigel, E. Freisinger and R. K. O. Sigel, De Gruyter, 2021, pp. 39–70.
2  J. Wahsner, E. M. Gale, A. Rodríguez-Rodríguez and P. Caravan, *Chem. Rev.*, 2019, **119**, 957–1057.
3  M. R. Prince, H. Zhang, Z. Zou, R. B. Staron and P. W. Brill, *American Journal of Roentgenology*, 2011, **196**, W138–W143.

4   B. Wagner, V. Drel and Y. Gorin, *American Journal of Physiology-Renal Physiology*, 2016, **311**, F1–F11.

5   B. J. Edwards, A. E. Laumann, B. Nardone, F. H. Miller, J. Restaino, D. W. Raisch, J. M. McKoy, J. A. Hammel, K. Bhatt, K. Bauer, A. T. Samaras, M. J. Fisher, C. Bull, E. Saddleton, S. M. Belknap, H. S. Thomsen, E. Kanal, S. E. Cowper, A. K. Abu Alfa and D. P. West, *BJR*, 2014, **87**, 20140307.

6   T. Grobner, *Nephrology Dialysis Transplantation*, 2006, **21**, 1104–1108.

7   P. Marckmann, L. Skov, K. Rossen, A. Dupont, M. B. Damholt, J. G. Heaf and H. S. Thomsen, *JASN*, 2006, **17**, 2359–2362.

8   M. Allard, D. Doucet, P. Kien, B. Bonnemain and J. M. Caillé, *Investigative Radiology*, 1988, **23**, S271–S274.

9   Z. Baranyai, F. Carniato, A. Nucera, D. Horváth, L. Tei, C. Platas-Iglesias and M. Botta, *Chem. Sci.*, 2021, **12**, 11138–11145.

10  Z. Garda, E. Molnár, F. K. Kálmán, R. Botár, V. Nagy, Z. Baranyai, E. Brücher, Z. Kovács, I. Tóth and G. Tircsó, *Front. Chem.*, 2018, **6**, 232.

11  E. Molnár, N. Camus, V. Patinec, G. A. Rolla, M. Botta, G. Tircsó, F. K. Kálmán, T. Fodor, R. Tripier and C. Platas-Iglesias, *Inorg. Chem.*, 2014, **53**, 5136–5149.

12  E. M. Gale, I. P. Atanasova, F. Blasi, I. Ay and P. Caravan, *J. Am. Chem. Soc.*, 2015, **137**, 15548–15557.

13  G. Tircsó, M. Regueiro-Figueroa, V. Nagy, Z. Garda, T. Garai, F. K. Kálmán, D. Esteban-Gómez, É. Tóth and C. Platas-Iglesias, *Chem. Eur. J.*, 2016, **22**, 896–901.

14  C. Platas-Iglesias, M. Mato-Iglesias, K. Djanashvili, R. N. Muller, L. V. Elst, J. A. Peters, A. de Blas and T. Rodríguez-Blas, *Chem. Eur. J.*, 2004, **10**, 3579–3590.

15  A. Vágner, E. Gianolio, S. Aime, A. Maiocchi, I. Tóth, Z. Baranyai and L. Tei, *Chem. Commun.*, 2016, **52**, 11235–11238.

16  F. Lucio-Martínez, Z. Garda, B. Váradi, F. K. Kálmán, D. Esteban-Gómez, É. Tóth, G. Tircsó and C. Platas-Iglesias, *Inorg. Chem.*, 2022, **61**, 5157–5171.

17  F. K. Kálmán, A. Végh, M. Regueiro-Figueroa, É. Tóth, C. Platas-Iglesias and G. Tircsó, *Inorg. Chem.*, 2015, **54**, 2345–2356.

18  B. Váradi, N. Lihi, S. Bunda, A. Nagy, G. Simon, M. Kéri, G. Papp, G. Tircsó, D. Esteban-Gómez, C. Platas-Iglesias and F. K. Kálmán, *Inorg. Chem.*, 2022, **61**, 13497–13509.

19  V.-M. Mukkala, C. Sund, M. Kwiatkowski, P. Pasanen, M. Högberg, J. Kankare and H. Takalo, *HCA*, 1992, **75**, 1621–1632.

20  R. Negri, Z. Baranyai, L. Tei, G. B. Giovenzana, C. Platas-Iglesias, A. C. Bényei, J. Bodnár, A. Vágner and M. Botta, *Inorg. Chem.*, 2014, **53**, 12499–12511.

21  F. Yerly, K. I. Hardcastle, L. Helm, S. Aime, M. Botta and A. E. Merbach, *Chem. Eur. J.*, 2002, **8**, 1031.

22  S. Aime, A. Barge, A. Borel, M. Botta, S. Chemerisov, A. E. Merbach, U. Müller and D. Pubanz, *Inorg. Chem.*, 1997, **36**, 5104–5112.

23  Z. Baranyai, M. Botta, M. Fekete, G. B. Giovenzana, R. Negri, L. Tei and C. Platas-Iglesias, *Chem. Eur. J.*, 2012, **18**, 7680–7685.

24  L. Tei, Z. Baranyai, M. Botta, L. Piscopo, S. Aime and G. B. Giovenzana, *Org. Biomol. Chem.*, 2008, **6**, 2361.

25  R. Y. Tsien, *Biochemistry*, 1980, **19**, 2396–2404.

26  S. Avedano, L. Tei, A. Lombardi, G. B. Giovenzana, S. Aime, D. Longo and M. Botta, *Chem. Commun.*, 2007, 4726.

27  L. Zekany and I. Nagypal, in *Computational Methods for the Determination of Formation Constants*, ed. D. J. Leggett, Springer US, Boston, MA, 1985, pp. 291–353.

28  R. D. Hancock, G. Jackson and A. Evers, *J. Chem. Soc., Dalton Trans.*, 1979, 1384.

29  Z. Baranyai, Z. Pálinkás, F. Uggeri and E. Brücher, *Eur. J. Inorg. Chem.*, 2010, **2010**, 1948–1956.

30  L. Sarka, L. Burai and E. Brücher, *Chem. Eur. J.*, 2000, **6**, 719–724.

31  J.-C. G. Bünzli, *Chem. Rev.*, 2010, **110**, 2729–2755.

32  A. Bourdolle, M. Allali, J.-C. Mulatier, B. Le Guennic, J. M. Zwier, P. L. Baldeck, J.-C. G. Bünzli, C. Andraud, L. Lamarque and O. Maury, *Inorg. Chem.*, 2011, **50**, 4987–4999.

33  D. Guillaumont, H. Bazin, J.-M. Benech, M. Boyer and G. Mathis, *ChemPhysChem*, 2007, **8**, 480–488.

34 N. Alzakhem, C. Bischof and M. Seitz, *Inorg. Chem.*, 2012, **51**, 9343–9349.

35 K. Binnemans, *Coordination Chemistry Reviews*, 2015, **295**, 1–45.

36 W. DeW. Horrocks and D. R. Sudnick, *J. Am. Chem. Soc.*, 1979, **101**, 334–340.

37 A. Beeby, I. M. Clarkson, R. S. Dickins, S. Faulkner, D. Parker, L. Royle, A. S. De Sousa, J. A. G. Williams and M. Woods, *J. Chem. Soc., Perkin Trans. 2*, 1999, 493–504.

38 R. M. Supkowski and W. DeW. Horrocks, *Inorganica Chimica Acta*, 2002, **340**, 44–48.

39 C. Charpentier, J. Salaam, A. Nonat, F. Carniato, O. Jeannin, I. Brandariz, D. Esteban-Gomez, C. Platas-Iglesias, L. J. Charbonnière and M. Botta, *Chemistry A European J*, 2020, **26**, 5407–5418.

40 R. K. Wilharm, M. V. Ramakrishnam Raju, J. C. Hoefler, C. Platas-Iglesias and V. C. Pierre, *Inorg. Chem.*, 2022, **61**, 4130–4142.

41 M. Mato-Iglesias, T. Rodríguez-Blas, C. Platas-Iglesias, M. Starck, P. Kadjane, R. Ziessel and L. Charbonnière, *Inorg. Chem.*, 2009, **48**, 1507–1518.

42 O. Porcar-Tost, J. A. Olivares, A. Pallier, D. Esteban-Gómez, O. Illa, C. Platas-Iglesias, É. Tóth and R. M. Ortuño, *Inorg. Chem.*, 2019, **58**, 13170–13183.

43 O. V. Yazyev, L. Helm, V. G. Malkin and O. L. Malkina, *J. Phys. Chem. A*, 2005, **109**, 10997–11005.

44 D. H. Powell, O. M. N. Dhubhghaill, D. Pubanz, L. Helm, Y. S. Lebedev, W. Schlaepfer and A. E. Merbach, *J. Am. Chem. Soc.*, 1996, **118**, 9333–9346.

45 S. Laurent, L. V. Elst and R. N. Muller, *Contrast Media Mol Imaging*, 2006, **1**, 128–137.

46 M. Rohrer, H. Bauer, J. Mintorovitch, M. Requardt and H.-J. Weinmann, *Investigative Radiology*, 2005, **40**, 715–724.

47 L. Helm, A. E. Merbach and É. Tóth, Eds., *The chemistry of contrast agents in medical magnetic resonance imaging*, John Wiley & Sons Inc, Hoboken, NJ, Second edition., 2013.

48 T. J. Swift and R. E. Connick, *The Journal of Chemical Physics*, 1962, **37**, 307–320.

49 T. J. Swift and R. E. Connick, *The Journal of Chemical Physics*, 1964, **41**, 2553–2554.

50 H. Lammers, F. Maton, D. Pubanz, M. W. van Laren, H. van Bekkum, A. E. Merbach, R. N. Muller and J. A. Peters, *Inorg. Chem.*, 1997, **36**, 2527–2538.

51 P. Caravan, D. Esteban-Gómez, A. Rodríguez-Rodríguez and C. Platas-Iglesias, *Dalton Trans.*, 2019, **48**, 11161–11180.

52 G. Nizou, E. Molnár, N. Hamon, F. K. Kálmán, O. Fougère, O. Rousseaux, D. Esteban-Gòmez, C. Platas-Iglesias, M. Beyler, G. Tircsó and R. Tripier, *Inorg. Chem.*, 2021, **60**, 2390–2405.

53 A. Rodríguez-Rodríguez, D. Esteban-Gómez, A. de Blas, T. Rodríguez-Blas, M. Fekete, M. Botta, R. Tripier and C. Platas-Iglesias, *Inorg. Chem.*, 2012, **51**, 2509–2521.

54 Z. Pálinkás, A. Roca-Sabio, M. Mato-Iglesias, D. Esteban-Gómez, C. Platas-Iglesias, A. de Blas, T. Rodríguez-Blas and É. Tóth, *Inorg. Chem.*, 2009, **48**, 8878–8889.

55 D. Esteban-Gómez, A. de Blas, T. Rodríguez-Blas, L. Helm and C. Platas-Iglesias, *ChemPhysChem*, 2012, **13**, 3640–3650.

56 H. M. Irving, M. G. Miles and L. D. Pettit, *Analytica Chimica Acta*, 1967, **38**, 475–488.

57 A. Chauvin, F. Gumy, D. Imbert and J. G. Bünzli, *Spectroscopy Letters*, 2004, **37**, 517–532.

58 *Spectroscopy Letters*, 2007, **40**, 193–193.

59 Frisch, M. J.; Trucks, G. W.; Schlegel, H. B.; Scuseria, G. E.; Robb, M. A.; Cheeseman, J. R.; Scalmani, G.; Barone, V.; Mennucci, B.; Petersson, G. A.; Nakatsuji, H.; Caricato, M.; Li, X.; Hratchian, H. P.; Izmaylov, A. F.; Bloino, J.; Zheng, G.; Sonnenberg, J. L.; Hada, M.; Ehara, M.; Toyota, K.; Fukuda, R.; Hasegawa, J.; Ishida, M.; Nakajima, T.; Honda, Y.; Kitao, O.; Nakai, H.; Vreven, T.; Montgomery Jr., J. A.; Peralta, J. E.; Ogliaro, F.; Bearpark, M. J.; Heyd, J.; Brothers, E. N.; Kudin, K. N.; Staroverov, V. N.; Kobayashi, R.; Normand, J.; Raghavachari, K.; Rendell, A. P.; Burant, J. C.; Iyengar, S. S.; Tomasi, J.; Cossi, M.; Rega, N.; Millam, N. J.; Klene, M.; Knox, J. E.; Cross, J. B.; Bakken, V.; Adamo, C.; Jaramillo, J.; Gomperts, R.; Stratmann, R. E.; Yazyev, O.; Austin, A. J.; Cammi, R.; Pomelli, C.; Ochterski, J. W.; Martin, R. L.; Morokuma, K.; Zakrzewski, V. G.; Voth, G. A.; Salvador, P.; Dannenberg, J. J.; Dapprich, S.; Daniels, A. D.; Farkas, Ö.; Foresman, J. B.; Ortiz, J. V.; Cioslowski, J.; Fox, D. J. Gaussian 09, Gaussian, Inc.: Wallingford, CT, USA, 2009., .

60 H. Schröder, A. Creon and T. Schwabe, *J. Chem. Theory Comput.*, 2015, **11**, 3163–3170.

61 J. Tao, J. P. Perdew, V. N. Staroverov and G. E. Scuseria, *Phys. Rev. Lett.*, 2003, **91**, 146401.

62 V. N. Staroverov, G. E. Scuseria, J. Tao and J. P. Perdew, *The Journal of Chemical Physics*, 2003, **119**, 12129–12137.

63 D. Andrae, U. Häußermann, M. Dolg, H. Stoll and H. Preuß, *Theoret. Chim. Acta*, 1990, **77**, 123–141.

64 M. Dolg, H. Stoll, A. Savin and H. Preuss, *Theoret. Chim. Acta*, 1989, **75**, 173–194.

65 J. Tomasi, B. Mennucci and R. Cammi, *Chem. Rev.*, 2005, **105**, 2999–3094.

66 F. Neese, *WIREs Comput Mol Sci*, , DOI:10.1002/wcms.1606.

67 D. Aravena, F. Neese and D. A. Pantazis, *J. Chem. Theory Comput.*, 2016, **12**, 1148–1156.

68 F. Weigend and R. Ahlrichs, *Phys. Chem. Chem. Phys.*, 2005, **7**, 3297.

69 D. A. Pantazis, X.-Y. Chen, C. R. Landis and F. Neese, *J. Chem. Theory Comput.*, 2008, **4**, 908–919.

70 F. Neese, F. Wennmohs, A. Hansen and U. Becker, *Chemical Physics*, 2009, **356**, 98–109.

71 R. Izsák and F. Neese, *The Journal of Chemical Physics*, 2011, **135**, 144105.

72 G. L. Stoychev, A. A. Auer and F. Neese, *J. Chem. Theory Comput.*, 2017, **13**, 554–562.

73 D. S. Raiford, C. L. Fisk and E. D. Becker, *Anal. Chem.*, 1979, **51**, 2050–2051.

74 S. Meiboom and D. Gill, *Review of Scientific Instruments*, 1958, **29**, 688–691.

75 H. Y. Carr and E. M. Purcell, *Phys. Rev.*, 1954, **94**, 630–638.

76 Y. Cohen, L. Avram and L. Frish, *Angew. Chem. Int. Ed.*, 2005, **44**, 520–554.

77 R. Mills, *J. Phys. Chem.*, 1973, **77**, 685–688.